

# Catalytic Decomposition of Gaseous SO<sub>3</sub>

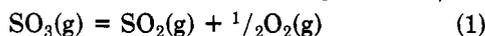
R. D. Brittain\* and D. L. Hildenbrand

SRI International, Menlo Park, California 94025 (Received: December 20, 1982)

The effectiveness of a number of potential catalysts for the process  $\text{SO}_3 \rightarrow \text{SO}_2 + 1/2\text{O}_2$  was studied by admitting gaseous  $\text{SO}_3$  to an alumina reactor containing the material and monitoring the exit gas composition by mass spectrometry. Measurements were made over the range 600–1000 K, at initial  $\text{SO}_3$  pressures of about  $1 \times 10^{-6}$  atm. Several metal and metal oxide powders found to be effective catalysts for  $\text{MgSO}_4$  decomposition were also found to catalyze  $\text{SO}_3$  decomposition, although there was a considerable spread in the onset temperatures of catalytic activity; these ranged from about 600 K for Pt and Ru to about 850 K for CoO. The metal oxides are effective only over the region in which the corresponding sulfates are unstable. The results offer an insight to the lack of catalytic activity of the oxides toward other metal sulfates.

## Introduction

In studies of the thermal decomposition of magnesium sulfate by the effusion method at about 1000 K,<sup>1</sup>  $\text{SO}_3$  was observed as the sole gaseous reaction product for the larger effusion orifices, although  $\text{SO}_2$  and  $\text{O}_2$  would be the dominant products at equilibrium, with  $P(\text{SO}_2)/P(\text{SO}_3) \sim 100$ . Likewise in effusion studies of the zinc sulfate<sup>2</sup> and copper sulfate<sup>3</sup> systems at about 850 and 750 K, respectively,  $\text{SO}_3$  was found to be the primary gaseous decomposition product, although  $\text{SO}_2$  and  $\text{O}_2$  would still be favored at equilibrium. Clearly there is a substantial barrier to the  $\text{SO}_3$  reduction, reaction 1, so that the vaporization/de-



composition behavior of these systems is dominated by the nonequilibrium process yielding  $\text{SO}_3$ .

In subsequent investigations<sup>4</sup> of the nature of this kinetic barrier, we studied the catalytic effects of several metals and metal oxides on the decomposition of magnesium sulfate, following the observation of Pechkovsky<sup>5</sup> that small additions of  $\text{Fe}_2\text{O}_3$  and  $\text{CuO}$  (but not  $\text{SiO}_2$ ) markedly accelerated its decomposition. The presence of some of these additives at levels of several mole percent led to the evolution of only  $\text{SO}_2$  and  $\text{O}_2$  from the sulfate and to higher decomposition pressures consistent with equilibrium behavior.<sup>4</sup> These results suggested a mechanism involving  $\text{SO}_3$  emission as the primary lattice decomposition step, followed by the near-equilibrium conversion of  $\text{SO}_3$  to  $\text{SO}_2$  and  $\text{O}_2$  only in the presence of a suitable catalyst for that process. As expected, it was found that the decomposition rate of  $\text{MgSO}_4$  was accelerated only when the catalytic additive was mixed intimately with the sulfate powder, so that  $\text{SO}_3$  reduction on surfaces of the additive could be coupled closely with the decomposition of the lattice sulfate ion. However, platinum was the only additive found to accelerate the decomposition of zinc sulfate,<sup>2</sup> while none of the additives effective at increasing the decomposition rate of  $\text{MgSO}_4$  had such an effect on copper sulfate or basic copper sulfate.<sup>3</sup> It is important to note, however, that while platinum did not catalyze the decomposition of  $\text{CuSO}_4$  or  $\text{CuO}\cdot\text{CuSO}_4$ , it did convert the effusing gas to  $\text{SO}_2$  and  $\text{O}_2$ .

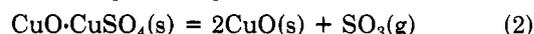
In order to verify that the additives accelerating  $\text{MgSO}_4$  decomposition are indeed effective catalysts for the reduction of  $\text{SO}_3$ , we have undertaken a brief study of the catalytic decomposition of  $\text{SO}_3$  in the absence of bulk metal sulfate so that the  $\text{SO}_3$  decomposition step may be decoupled from the sulfate lattice decomposition step. A second objective was to determine the temperature range of effective catalytic activity, so as to gain insight into the drastically different effects of the various catalytic additives on the different metal sulfate systems. The studies were carried out by admitting gaseous  $\text{SO}_3$  from an external source into an inert reactor containing the catalytic additive to be studied and monitoring the  $\text{SO}_3$  pressure in the catalyst chamber by mass spectrometry. The initial  $\text{SO}_3$  pressure was about  $1 \times 10^{-6}$  atm, typical of the effusion cell pressures in earlier sulfate decomposition studies.<sup>1-4</sup>

## Experimental Section

$\text{SO}_3(\text{g})$  was generated by decomposition of basic copper sulfate in a 2.5-cm-diameter cylindrical glass bulb surrounded by a resistance heater. The gas passed upward through a 0.6-cm-diameter silica tube into a Knudsen cell reactor positioned before the entrance slit of a quadrupole mass filter. As shown in Figure 1,  $\text{SO}_3$  molecules entering the alumina reactor encountered an alumina disk which forced multiple collisions with the catalyst sample before escape of the product gas through the cell orifice. The cell reactor was heated by a spiral wound molybdenum heater and the temperature was detected by a Pt-Pt-13% Rh thermocouple attached to the outside surface by an adjustable platinum band. An alumina cylinder positioned inside the heater minimized decomposition of emitted  $\text{SO}_3$  on the heater surface.

The partial pressure of  $\text{SO}_3$  effusing from the reactor was monitored by an Extranuclear quadrupole mass filter with a mass range of 800 amu. Ions emerging from the axial ionizer passed through the mass filter and were detected by a 21-stage Cu-Be multiplier. Pumping of the reactor and mass filter was provided by a 6-in. mercury diffusion pump. In order to minimize decomposition of the highly reactive  $\text{SO}_3$  in the ion source, the stainless steel entrance aperture plate was replaced by an alumina plate of the same dimensions. A movable beam-defining slit between the reactor orifice and the ionizer permitted the separation of sample and background components of the  $\text{SO}_3^+$  signal.

Basic copper sulfate,  $\text{CuO}\cdot\text{CuSO}_4$ , which yields  $\text{SO}_3$  by the thermal decomposition process



provided a stable and reliable source of  $\text{SO}_3$  for the catalysis experiments. We have studied the decomposition of

(1) Lau, K. H.; Cubicciotti, D.; Hildenbrand, D. L. *J. Chem. Phys.* 1977, 66, 4532-9.

(2) Lau, K. H.; Knittel, D. R.; Brittain, R. D.; Hildenbrand, D. L., to be submitted to *J. Phys. Chem.*

(3) Brittain, R. D.; Lau, K. H.; Hildenbrand, D. L., to be submitted to *J. Phys. Chem.*

(4) Knittel, D. R.; Lau, K. H.; Hildenbrand, D. L. *J. Phys. Chem.* 1980, 84, 1890-4.

(5) Pechkovsky, V. V. *J. Appl. Chem. USSR (Engl. Transl.)* 1956, 29, 1229.

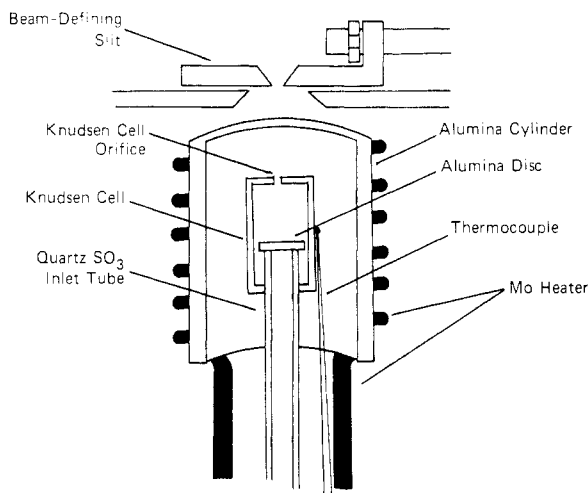


**Figure 1.** Knudsen cell reactor and heater assembly for  $\text{SO}_3$  decomposition experiments.

basic copper sulfate by torsion-effusion and mass spectrometry,<sup>3</sup> finding that  $\text{SO}_3$  is the primary decomposition product, although  $\text{SO}_2$  and  $\text{O}_2$  comprise as much as 20% of the vapor after partial decomposition, indicating that the presence of  $\text{CuO}$  may promote the decomposition of  $\text{SO}_3$ . Since we are monitoring changes in the intensity of  $\text{SO}_3$  effusing from the reactor and are limiting our experiments to the initial stage of basic sulfate decomposition, our results will not be affected. The vapor pressure of  $\text{SO}_3$  above basic copper sulfate, as measured by torsion-effusion studies, is described by

$$\log P(\text{atm}) = 10.561 - \frac{12790}{T(\text{K})} \quad (3)$$

Basic copper sulfate was prepared by decomposition of anhydrous copper sulfate in air at 1000 K. The sample bulb of the gas inlet system was loaded with 10–20 g of the basic sulfate and heated for several hours at 770 K while the product gas was monitored with the mass filter. During the initial warm-up, only  $\text{SO}_2^+$  and  $\text{O}_2^+$  were observed, but after several hours of conditioning by passing  $\text{SO}_3$  through the system, the  $\text{SO}_2^+$  and  $\text{O}_2^+$  signals decreased to low levels and the  $\text{SO}_3^+$  signal reached a stable level. Following the initial run with a fresh sample of basic copper sulfate, conditioning was not necessary and  $\text{SO}_3^+$  appeared immediately after the sample was warmed to an appropriate temperature. Apparently it was necessary to passivate the system initially by removal of adsorbed reactive gases before a stable  $\text{SO}_3$  flow could be maintained.  $\text{SO}_3$  was identified positively from the ionization efficiency curve of the parent ion at  $m/e$  80; the measured threshold appearance potential was 13.0 eV, compared to a first IP of 12.81 eV determined by photoelectron spectroscopy.<sup>6</sup>

The pressure relation expressed in eq 3 was employed in converting the  $\text{SO}_3^+$  signals into absolute pressure units. For this purpose the Knudsen cell reactor was loaded with a sample of basic copper sulfate and the  $\text{SO}_3^+$  signal was followed as a function of the reactor temperature. With the calibration data so derived, the  $\text{SO}_3^+$  signal was related to  $\text{SO}_3$  pressure during catalysis runs. Quadrupole instrument settings remained constant throughout the experiments and similar calibration runs at the conclusion showed that  $\text{SO}_3^+$  sensitivity was a constant.

An identical procedure was followed in all  $\text{SO}_3$  decomposition runs. Approximately 50 mg of the sample to be

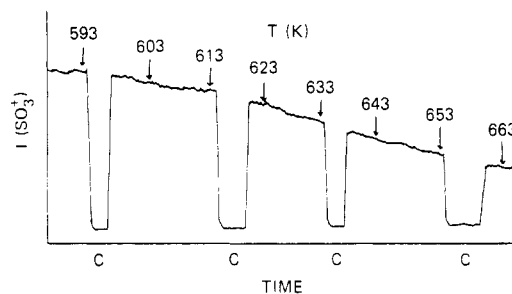


**Figure 2.** Typical chart recording of  $\text{SO}_3$  decomposition run with Pt catalyst. C indicates that the beam-defining slit is closed.

studied for catalytic activity was loaded around the gas inlet tube and on top of the alumina disk in the reactor, and the system was evacuated slowly to avoid disturbing the sample. After the system pressure was less than  $1 \times 10^{-7}$  atm, the reactor was heated to 600 K. The temperature of the basic copper sulfate sample was raised until a stable  $\text{SO}_3^+$  signal corresponding to the desired pressure (usually  $1 \times 10^{-6}$  atm) was observed. The reactor temperature was then raised to 900 K to remove adsorbed gases from sample surfaces while  $\text{SO}_3$  flow was maintained. The  $\text{SO}_3^+$  signal was observed carefully during this initial heating so that the approximate onset of  $\text{SO}_3$  decomposition could be determined. Beginning at a stable temperature 10–20 K below the onset temperature, and after the  $\text{SO}_3^+$  signal stabilized, the voltage applied to the molybdenum heater was adjusted periodically to maintain a heating rate of 2–4 K/min. Lower heating rates did not affect the results. The  $\text{SO}_3^+$  signal was recorded continuously during each run and the background component of the signal was checked at intervals of 20–30 K by displacement of the beam-defining slit. The chart recording of a typical run with a platinum sample is reproduced in Figure 2. Blank runs performed without catalyst in the cell showed that there was no observable  $\text{SO}_3$  decomposition below 950 K, and about 50% decomposition at 1050 K. Below 600 K,  $\text{SO}_3$  apparently reacted with the cell to form an aluminum sulfate, limiting catalytic studies to the range 600–1000 K. In the cases of platinum and chromium oxide, the pressure dependence of the catalytic activity was also investigated.

Samples investigated in this study were taken from the same batches prepared for  $\text{MgSO}_4$  decomposition studies reported earlier<sup>4</sup> with the exception of the  $\text{V}_2\text{O}_4$  sample, obtained from Alfa Products.

## Results

**Catalysis at  $1 \times 10^{-6}$  atm.** The activity of ten potential catalysts was investigated at initial  $\text{SO}_3$  pressures of approximately  $1 \times 10^{-6}$  atm. At least two runs were made on each sample to check the reproducibility of the data. The results are summarized in Table I, which shows the percentage decomposition of  $\text{SO}_3$  as a function of temperature for each catalyst, as compared to a blank run with no catalyst present and to the equilibrium composition at  $1 \times 10^{-6}$  atm. The lowest threshold temperatures for catalysis were exhibited by Pt and Ru, about 40 K above the equilibrium condition; the metal oxides became effective at progressively higher temperatures, with ZnO being only slightly more active than the cell assembly itself.

Successive runs on each catalyst generally exhibited highly reproducible  $\text{SO}_3$  decomposition behavior. With the ruthenium sample, however, the temperature for 50% decomposition at  $1 \times 10^{-6}$  atm was shifted upward by about 50 K after a run was performed at an initial pressure of  $4 \times 10^{-6}$  atm. The shift in temperature indicates a change in the condition of the ruthenium sample surface;

(6) Alderdice, D. S.; Dixon, R. N. *J. Chem. Soc., Faraday Trans. 2* 1976, 72, 372–8.

TABLE I: Temperatures for Various Decomposition Levels of SO<sub>3</sub> in the Presence of Catalysts

system	% SO <sub>3</sub> decomposed <sup>a</sup>									
	0	10	20	30	40	50	60	70	80	90
equilibrium	<400	526	556	574	592	610	624	642	664	697
Ru	593	605	620	629	639	648	662	672	688	713
Pt	593	613	620	635	644	653	665	678	695	733
V <sub>2</sub> O <sub>4</sub>	643	707	718	733	748	756	765	776	783	
CuO	753	776	787	793	800	805	811	820	832	848
Cr <sub>2</sub> O <sub>3</sub>	763	779	789	804	812	825	839	850	865	893
Fe <sub>2</sub> O <sub>3</sub>	793	815	823	835	841	845	850	855	863	883
NiO	843	852	858	864	869	875	881	888	896	903
Mn <sub>3</sub> O <sub>4</sub>	843	855	866	871	877	884	890	904	919	939
CoO	853	856	860	865	874	885	892	899	916	
ZnO				1005	1015	1021	1036	1044		
blank (Al <sub>2</sub> O <sub>3</sub> + SiO <sub>2</sub> )	870	935	969	1008	1039	1063	1088	1113	1141	

<sup>a</sup> At initial SO<sub>3</sub> pressure = 1 × 10<sup>-6</sup> atm.

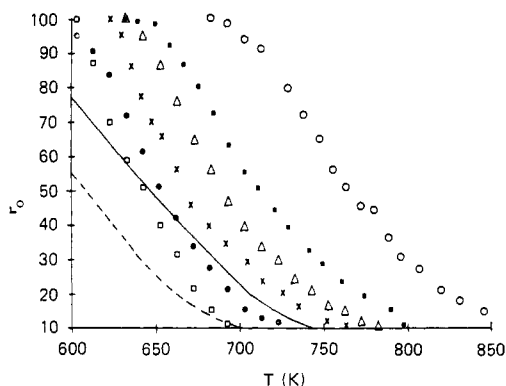


Figure 3. Pressure dependence of SO<sub>3</sub> decomposition catalysis by Pt.  $P_{\text{SO}_3}$  (atm) × 10<sup>6</sup>: □, 0.11; ●, 1.0; ×, 3.0; △, 6.5; ■, 25; ○, 88; —, equilibrium ( $P_T = 1 \times 10^{-6}$  atm); ---- equilibrium ( $P_T = 1 \times 10^{-5}$  atm).

oxidation may occur at higher temperatures. Less pronounced degradation of catalytic activity was observed in the cases of Fe<sub>2</sub>O<sub>3</sub>, Cr<sub>2</sub>O<sub>3</sub>, and V<sub>2</sub>O<sub>4</sub>, with shifts of 15, 18, and 40 K, respectively, in successive runs at  $P(\text{SO}_3) = 1 \times 10^{-6}$  atm. For other samples studied, the reproducibility of decomposition behavior was excellent. It is doubtful that the observed shifts in decomposition behavior result from removal of absorbed gases or the reduction of catalyst area by sintering, since the samples were preheated to 900 K before runs were commenced.

The data in Table I are taken from runs in which temperature increased at a constant rate. When the temperature was cycled, the SO<sub>3</sub><sup>+</sup> signal behavior was essentially reversible, but some hysteresis was observed; it took up to 1 h in some cases for the SO<sub>3</sub><sup>+</sup> signal to recover completely at the catalytic onset temperature. Repetition of the decomposition run after SO<sub>3</sub><sup>+</sup> signal recovery generally gave very reproducible results.

**Pressure Dependence of SO<sub>3</sub> Decomposition.** The pressure dependence of the platinum catalyst was investigated for initial SO<sub>3</sub> pressures in the ranges 1 × 10<sup>-7</sup> to 9 × 10<sup>-5</sup> atm. The decomposition curves for Pt catalysis at six different initial SO<sub>3</sub> pressures are shown in Figure 3, along with the equilibrium curves for 1 × 10<sup>-6</sup> and 1 × 10<sup>-5</sup> atm. It is observed that the onset of catalytic activity occurs at higher temperature when the initial SO<sub>3</sub> pressure is higher, the relative shift being comparable to the shift in the equilibrium curve. The temperature shift from equilibrium at each initial  $P(\text{SO}_3)$  is noted in Table II as  $\Delta T$ . The results of similar determination of the pressure dependence of Cr<sub>2</sub>O<sub>3</sub> catalysis are presented in Table III.

**Sulfation of Oxide Catalyst.** For the initial run on each catalyst, the sample was held at 600 K while an SO<sub>3</sub>(g) flow corresponding to an SO<sub>3</sub> pressure of 1 × 10<sup>-6</sup> atm in the cell reactor was established. The temperature of the

TABLE II: Temperatures for 50% SO<sub>3</sub> Decomposition at Equilibrium and in the Presence of Platinum

$P$ , atm	$T_{1/2}(\text{equil})$	$T_{1/2}(\text{Pt})$	$\Delta T$
1.1 × 10 <sup>-7</sup>	575	645	70
1.0 × 10 <sup>-6</sup>	608	653	45
3.0 × 10 <sup>-6</sup>	622	665	43
6.5 × 10 <sup>-6</sup>	639	690	51
2.5 × 10 <sup>-5</sup>	663	715	52
8.8 × 10 <sup>-5</sup>	686	770	84

TABLE III: Temperature for 50% SO<sub>3</sub> Decomposition at Equilibrium and in the Presence of Cr<sub>2</sub>O<sub>3</sub>

$P$ , atm	$T_{1/2}(\text{equil})$	$T_{1/2}(\text{Cr}_2\text{O}_3)$	$\Delta T$
3.0 × 10 <sup>-7</sup>	589	810	221
1.1 × 10 <sup>-6</sup>	609	827	218
1.7 × 10 <sup>-6</sup>	616	833	217
1.0 × 10 <sup>-5</sup>	645	850	205

catalyst sample was then raised while the SO<sub>3</sub><sup>+</sup> signal was observed. In studies of CuO, CoO, NiO, Fe<sub>2</sub>O<sub>3</sub>, and Mn<sub>3</sub>O<sub>4</sub>, the SO<sub>3</sub><sup>+</sup> signal increased significantly as the threshold temperature was approached, then decreased rapidly above the threshold temperature. We postulated that the SO<sub>3</sub><sup>+</sup> signal increased because metal sulfate, formed by SO<sub>3</sub> flow over the oxide catalysts at low temperature, decomposed near the threshold temperature. Several runs were required to establish the catalysis threshold temperature for these samples. For the data presented in Table I, each run was initiated after holding the temperature constant at the threshold point for several minutes, during which time the SO<sub>3</sub><sup>+</sup> signal was constant. Decomposition curves obtained by this procedure were reproducible.

In order to verify that sulfation occurred in the CuO sample, the SO<sub>3</sub> flow was held constant while the reactor temperature was lowered to 100 K below the threshold temperature; the SO<sub>3</sub><sup>+</sup> signal was observed to decrease by about 30%. The SO<sub>3</sub> flow was then terminated. When the reactor temperature was then increased at a constant rate, the SO<sub>3</sub><sup>+</sup> signal reappeared and rose to a maximum at the threshold temperature for CuO catalysis, indicating that copper sulfate formed by sulfation of the catalyst sample was undergoing decomposition.

## Discussion

The primary objective of this study was to determine whether catalytic additives effective in increasing the decomposition pressure of magnesium sulfate<sup>4</sup> were likewise effective in the reduction of SO<sub>3</sub> in the absence of bulk metal sulfate. In addition, we wished to examine the temperature dependence of catalytic activity to check for a correlation with the lack of catalysis of the zinc and copper sulfate decompositions.<sup>2,3</sup> Figure 4 is a plot of the

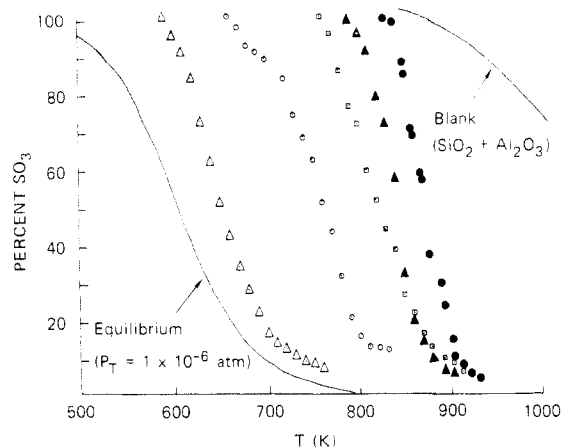


**Figure 4.** Catalyst effectiveness of ( $\Delta$ ) Pt, ( $\circ$ )  $V_2O_4$ , ( $\square$ )  $Cr_2O_3$ , ( $\blacktriangle$ )  $Fe_2O_3$ , and ( $\bullet$ ) NiO.

**TABLE IV:** Correlation of 50%  $SO_3$  Decomposition Temperatures with Catalyzed  $MgSO_4$  Decomposition Pressures

catalyst	$SO_3$ $T_{1/2}$ , K	$MgSO_4^a$ $P(\text{cat})/P(\text{uncat})$
Pt	653	59
Ru	648	10
$V_2O_4$	755	13
$Cr_2O_3$	825	27
$Fe_2O_3$	845	23
NiO	875	8
$Mn_3O_4$	884	14
CoO	885	15
ZnO	1030	2

<sup>a</sup> At 900–1000 K.

results of  $SO_3$  decomposition experiments on several of the metal and metal oxide catalysts at  $1 \times 10^{-6}$  atm. The percentage decomposition of  $SO_3$  as a function of temperature is compared to the equilibrium condition and to the blank run with no catalyst present. It is clear that not only are the catalysts effective in the absence of metal sulfate, but that there are also wide differences in the threshold temperatures for catalytic activity.

Consider first the implications of these results in the decomposition of magnesium sulfate. In Table IV results of catalysis of  $SO_3$  reduction by ten additives are summarized by the characteristic temperature,  $T_{1/2}$ , at which each additive decomposes 50% of the  $SO_3$  passing through the cell reactor at  $1 \times 10^{-6}$  atm. The results are compared with the effectiveness of the same catalysts for the decomposition of  $MgSO_4$ , as shown by the ratio  $P(\text{cat})/P(\text{uncat})$  in the third column. In all cases reported, the catalysts studied are effective in both  $SO_3$  reduction and  $MgSO_4$  decomposition, and a rough correlation is observed between  $T_{1/2}$  values for  $SO_3$  reduction and the relative decomposition pressure increases by the catalysts when added to  $MgSO_4$ . In the case of catalysis by ruthenium, the  $T_{1/2}$  value is about the same as that for platinum, while the ratio  $P(\text{cat})/P(\text{uncat})$  is six times greater for Pt than for Ru. The observed difference is explained in part by the increase in the  $T_{1/2}$  for Ru by 50 K following higher pressure runs with that catalyst. The reason for the degradation in Ru effectiveness is not understood, but may be related to oxidation or poisoning of sample surfaces. A revision will be noted for the value of  $P(\text{cat})/P(\text{uncat})$  for  $V_2O_4$ , which is now listed as 13 in Table IV, as remeasured with a commercial sample of  $V_2O_4$ . The value of 1.9 reported earlier<sup>4</sup> is for a run in which  $V_2O_4$  was prepared by thermal decomposition of  $V_2O_5$ , and the resulting  $V_2O_4$  was identified by X-ray diffraction analysis. The higher value

**TABLE V:** Catalyst Effectiveness in  $CuSO_4$  and  $ZnSO_4$  Decomposition and  $SO_3$  Reduction Processes

sulfate system	$T(P = 1 \times 10^{-6} \text{ atm})$ , K		decomposin catalysts	$SO_3$ reducun catalysis
		catalyst		
$CuSO_4$	710	Pt	no	yes
		CuO	no	yes
$CuO \cdot CuSO_4$	735	Pt	no	yes
$ZnSO_4$	740	Pt	yes	yes
$ZnO \cdot ZnSO_4$	800	Pt	yes	yes
		Ru	no	yes
		CuO	slight	no data
		$Cr_2O_3$	no	no data

of  $P(\text{cat})/P(\text{uncat})$  for the commercial sample is more in line with the observed effectiveness of  $V_2O_4$  in  $SO_3$  reduction. The correlation of results for the two types of reaction extends even to the ZnO additive, where, at 1000 K, ZnO causes only a doubling of  $MgSO_4$  decomposition pressure and less than 30% reduction of  $SO_3$  (Table I). The comparison in Table IV indicates that catalytic activity in  $SO_3$  reduction is a prerequisite for effective catalysis of the  $MgSO_4$  decomposition rate and the related increase in decomposition pressure.

With the comparison of the  $SO_3$  reduction and  $MgSO_4$  decomposition results as a guide, the results of catalytic decomposition experiments on the sulfates and basic sulfates of copper and zinc may be examined. From mass-loss torsion-effusion measurements reported on admixed samples of each sulfate system with selected catalysts, two types of information are available: (1) the average molecular weight of the effusing gas, and (2) the total pressure above the sample. An observed molecular weight of 80 indicates that only  $SO_3$  gas is present in the effusate, while a value of 55 corresponds to an equilibrium mixture of  $SO_2$  and  $O_2$ . Table V summarizes the results observed in catalytic experiments on the copper and zinc sulfates. The criterion for  $SO_3$  reduction catalysis as reported in Table V was an observed vapor molecular weight of 55, while an observed value of  $P(\text{cat})/P(\text{uncat})$  above 1.0 was required for classification as a catalyst in the sulfate decomposition process. Although not all possible catalyst-sulfate combinations were studied, the results available show that  $SO_3$  reduction is indeed observed for all systems studied. Increases in decomposition pressure are observed only in selective cases, however, specifically in mixtures of Pt or CuO with basic zinc sulfate or of platinum with zinc sulfate. CuO had only marginal effects on the decomposition pressure of  $ZnO \cdot 2ZnSO_4$ , as might be expected, since catalytic reduction of  $SO_3$  is only partially complete at 800 K (Table I). We may then conclude that the capability of a catalyst for  $SO_3$  reduction is not a sufficient condition for catalyzing the decomposition of a metal sulfate.

Another necessary condition may be that the rate of surface diffusion of  $SO_3$  across the product oxide boundary to the catalyst surface must be rapid. If this rate is sufficiently temperature dependent, then the lattice decomposition and  $SO_3$  reduction steps may be decoupled at the lower temperatures, in accord with the lack of catalytic activity of Pt on decomposition of the copper sulfates.

The observed sulfation of certain oxide catalysts in the  $SO_3$  reduction experiments is strongly correlated with the onset of reduction catalysis. In Table VI the temperatures of catalysis threshold for  $SO_3$  reduction are compared with the known temperatures<sup>7</sup> at which the decomposition pressures of corresponding sulfates reach  $1 \times 10^{-6}$  atm. For

(7) Kellog, H. H. *Trans. Metall. Soc. AIME* 1964, 230, 1622–34.

TABLE VI: Comparison of Sulfate Decomposition<sup>a</sup> and Catalysis Onset Temperatures

metal sulfate	$T(P_d = 1 \times 10^{-6} \text{ atm}), \text{ K}$	catalyst	$T(\text{onset}), \text{ K}$
CuSO <sub>4</sub>	710	CuO	760
CuO·CuSO <sub>4</sub>	730		
Fe <sub>2</sub> (SO <sub>4</sub> ) <sub>3</sub>	640	Fe <sub>2</sub> O <sub>3</sub>	800
NiSO <sub>4</sub>	790	NiO	830
CoSO <sub>4</sub>	825	CuO	860

<sup>a</sup> Calculated from data in ref 7.

the copper, nickel, and cobalt systems, SO<sub>3</sub> reduction becomes possible close to the temperature at which the sulfate becomes thermodynamically unstable. In the Fe-S-O system, however, there are no known sulfate phases above 640 K under these conditions, but catalytic activity is observed only above 800 K. The decomposition temperature of the corresponding sulfate then sets a lower limit on the temperature at which a metal oxide can become an effective catalyst in SO<sub>3</sub> reduction, but other factors such as the ability of the oxide to chemisorb oxygen also may play an important role in determining catalytic effectiveness.

Close correspondence between sulfate decomposition and catalysis threshold temperatures has significance in studies of sulfate decomposition processes, because the establishment of a solid product phase which catalytically reduces SO<sub>3</sub> from the sulfate lattice will then affect the gas composition and possibly the rate of decomposition of the sulfate. Mass spectrometric and vapor molecular

weight information from our study<sup>3</sup> of copper sulfate and basic copper sulfate decomposition processes clearly demonstrates that SO<sub>3</sub> is the dominant (>90%) gaseous decomposition product when less than 1% of the sample has decomposed. In later stages of the experiments, however, the vapor composition changes to mostly SO<sub>2</sub> and O<sub>2</sub>; the nucleation of a CuO product phase in the decomposing sulfate samples provides catalytically active surfaces on which SO<sub>3</sub> may decompose, consistent with our observations here of CuO catalytic activity above 750 K. However, the observed pressures are relatively independent of the degree of decomposition of the sample, so that reduction of SO<sub>3</sub> is not so closely coupled with the lattice decomposition step that sulfate decomposition catalysis occurs. In contrast to the results for the copper system, SO<sub>3</sub> is the dominant gas-phase product of the decomposition of both zinc sulfate and basic zinc sulfate even after significant decomposition, as would be expected considering the relatively low degree of catalytic activity observed with ZnO. We intend to investigate the decomposition of iron, nickel, and cobalt sulfates in order to test the validity of this model in other systems where the reaction product phase may act as a "built-in" catalyst.

*Acknowledgment.* This work was supported by the Office of Basic Energy Sciences, U.S. Department of Energy.

**Registry No.** SO<sub>3</sub>, 7446-11-9; Ru, 7440-18-8; Pt, 7440-06-4; VO<sub>2</sub>, 12036-21-4; CuO, 1317-38-0; Cr<sub>2</sub>O<sub>3</sub>, 1308-38-9; Fe<sub>2</sub>O<sub>3</sub>, 1309-37-1; NiO, 1313-99-1; Mn<sub>2</sub>O<sub>4</sub>, 1317-35-7; CoO, 1307-96-6; ZnO, 1314-13-2.

## Photochemistry of Methyl Viologen in Aqueous and Methanolic Solutions

T. W. Ebbesen\* and G. Ferraudi

Radiation Laboratory, University of Notre Dame, Notre Dame, Indiana 46556 (Received: December 20, 1983)

The photochemistry of MV<sup>2+</sup>(Cl<sup>-</sup>)<sub>2</sub> (methyl viologen; paraquat; 1,1'-dimethyl-4,4'-bipyridinium dichloride) has been investigated in both H<sub>2</sub>O and CH<sub>3</sub>OH. It is shown that the observed photochemistry occurs via the ground-state charge-transfer complexation with the halide counterion(s). In H<sub>2</sub>O, the radical pair MV<sup>•+</sup>·Cl<sub>2</sub><sup>-•</sup> is formed with a quantum yield of 0.2 from the dichloride complex ( $K_{2\text{Cl}} = 1.4 \text{ M}^{-1}$ ) with a rate  $>10^8 \text{ s}^{-1}$ . The MV<sup>•+</sup>·Cl<sub>2</sub><sup>-•</sup> formation and decay is pH independent (1.5 to 9), the kinetics of the disappearance being second order. When the Cl<sup>-</sup> counterions are replaced by Br<sup>-</sup> ( $K_{2\text{Br}} = 1.8 \text{ M}^{-1}$ ) or by I<sup>-</sup> ( $K_{2\text{I}} = 3.2 \text{ M}^{-1}$ ) the quantum yield drops dramatically (<0.01). By comparison with Cs<sup>+</sup> it is concluded that an intracomplex heavy-atom effect is observed. In methanol, where the end product is MV<sup>•+</sup>·Cl<sup>-</sup>, it is shown that the radical pair MV<sup>•+</sup>·Cl<sup>-</sup> must be an intermediate in the formation of the initial methoxy radical and MV<sup>•+</sup>, the observed quantum yield of the latter being strongly dependent on the chloride concentration. Furthermore, in agreement with previous suggestions in the literature, the results indicate that a weak methyl viologen chloride-methanol complex is involved in the MV<sup>2+</sup>(Cl<sup>-</sup>)<sub>2</sub> photochemistry in methanol.

### Introduction

In view of the wide interest in and usage of methyl viologen (paraquat; 1,1'-dimethyl-4,4'-bipyridinium dichloride; MV<sup>2+</sup>(Cl<sup>-</sup>)<sub>2</sub>) as an intermediate in systems designed for solar energy conversion,<sup>1</sup> as an herbicide,<sup>2</sup> and

as an electron acceptor in charge-transfer complexes,<sup>3</sup> it is most important to understand its *own* photochemistry. The main photochemical studies of MV<sup>2+</sup>(Cl<sup>-</sup>)<sub>2</sub> have been

(1) See, for example: Johansen, O.; Launikonis, A.; Loder, J. W.; Mau, A. W. H.; Sasse, W. H. F.; Swift, J. D.; Wells, D. *Aust. J. Chem.* 1981, 34, 981-91. Chan, S. F.; Chou, M.; Creutz, C.; Matsubara, T.; Sutin, N. *J. Am. Chem. Soc.* 1981, 103, 369-79. Kirch, M.; Lehn, J. M.; Sauvage, J. P. *Helv. Chem. Acta* 1979, 62, 1345-84. Kalyanasundaram, K.; Gratzel, L. *Ibid.* 1980, 63, 478-85. Harriman, A.; Porter, G.; Richoux, M. C.; *J. Chem. Soc., Faraday Trans. 2* 1981, 77, 833-44. Rougee, M.; Ebbesen, T. W.; Ghetti, F.; Bensasson, R. *J. Phys. Chem.* 1982, 86, 4404-12.

(2) See, for example: Dodge, A. D. *Endeavour* 1971, 30, 130-5. Farrington, J. A.; Ebert, M.; Land, E. J.; Fletcher, K. *Biochim. Biophys. Acta* 1973, 314, 372-81. Nanni, E. J.; Angelis, C. T.; Dickson, J.; Sawyer, D. T. *J. Am. Chem. Soc.* 1981, 103, 4268-70. Levey, G.; Rieger, A. L.; Edwards, J. O. *J. Org. Chem.* 1981, 46, 1255-60. Levey, G.; Ebbesen, T. W. *J. Phys. Chem.* 1983, 87, 829-32.

(3) See, for example: Poulos, A. T.; Kelley, C. K.; Simone, R. *J. Phys. Chem.* 1981, 85, 823-8. Deronzier, A. *J. Chem. Soc., Chem. Commun.* 1982, 329-31. Sullivan, E. P.; Dressick, W. J.; Meyer, T. *J. Phys. Chem.* 1982, 86, 1473-8. Andrade de Oliveira, L. A.; Haim, A. *J. Am. Chem. Soc.* 1982, 104, 3363-6.